

Comparison of System Identification Techniques in the Analysis of a Phantom for Studying Shaken-baby Syndrome

Thomas O. Lintern, Mark C. Finch, Andrew J. Taberner, Poul M. F. Nielsen and Martyn P. Nash

Abstract—This article compares two techniques for estimating the parameters describing the motion of a phantom designed to investigate shaking baby syndrome. Parameters of a simple computational model and an impulse response function for a linear second order system were both fitted using kinematic measurements of the motion of an inverted jointed pendulum. From the two methods respectively, the rotational stiffness of the joint was calculated to be $1.396 \text{ kgm}^2\text{s}^{-2}$ and $1.355 \text{ kgm}^2\text{s}^{-2}$ and the damping coefficient was calculated to be $0.0142 \text{ kgm}^2\text{s}^{-1}$ and $0.0133 \text{ kgm}^2\text{s}^{-1}$. The parameter estimates were similar demonstrating that the two techniques were comparable. Identifying accurate parameters will allow more complex phantoms to be modeled, and will provide insight into the relationship between the shaking of the torso and the resultant head motion during shaken baby syndrome.

I. INTRODUCTION

SHAKEN Baby Syndrome (SBS), the abusive shaking of infants resulting in injury or death, occurs at a rate of 20-30 cases per 100,000 infants worldwide [1]-[5]. Diagnosis of SBS is subjective and there is debate about whether shaking is in fact responsible for the injuries often attributed to SBS [6]-[9]. Some research [8] suggests that the patterns of injury – subdural and/or retinal haemorrhaging and a lack of any external abrasions – are in fact due to a physiological cascade of events that *may* be benign in origin. The controversy surrounding SBS has resulted in legal disputes [10] with experts being required to express confident opinions in a field where little objective evidence exists. It is therefore important to provide clinicians with an objective and quantitative tool to relate motions of the head to motions subjected to the infant by a parent or caregiver.

The aim of this project is to use kinematic modelling and experimentation to predict the motion of a phantom in response to controlled input accelerations. The phantom

Manuscript received April 15, 2011. This work was supported by The Health Research Council of New Zealand via a Maori Career Development PhD Scholarship for Thomas Lintern.

T. O. Lintern is with the Auckland Bioengineering Institute at The University of Auckland (phone: +64 9 373 7599; fax: +64 9 367 7157 ; e-mail: tlin067@aucklanduni.ac.nz).

M. C. Finch is with the Auckland Bioengineering Institute at The University of Auckland (e-mail: m.finch@auckland.ac.nz).

A. J. Taberner is with the Auckland Bioengineering Institute and the Department of Engineering Science at The University of Auckland (e-mail: a.taberner@auckland.ac.nz).

P. M. F. Nielsen is with the Auckland Bioengineering Institute and the Department of Engineering Science at The University of Auckland (e-mail: p.nielsen@auckland.ac.nz).

M. P. Nash is with the Auckland Bioengineering Institute and the Department of Engineering Science at The University of Auckland (e-mail: martyn.nash@auckland.ac.nz).

attempts to recreate the anatomy and behaviour of an existing animal model being subjected to different shaking protocols, consisting of a multi-link inverted pendulum, representing the neck's articulated structure. To describe the kinematics of a multi-link phantom, it is first important to characterise the properties of a single joint. This paper presents two methods for identifying the stiffness and damping of a single joint phantom system.

II. PHANTOM

A simple inverted pendulum was constructed consisting of a plastic rod mounted on an actuation stage via a rubber joint of unknown rotational stiffness (Fig. 1). The actuation was provided by a linear motor (ServoTube, Copley Controls, U.S.A). Kinematic measurements of the pendulum's motion were provided by a wireless inertial sensor, mounted at the top of the pendulum. The sensor (developed in our laboratory in collaboration with Telemetry Research Ltd) is

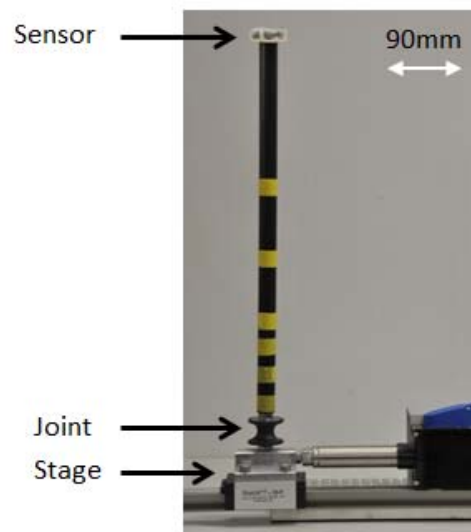


Fig. 1. Inverted Pendulum Phantom including sensor (top), pendulum rod, rubber joint and actuation stage.

capable of measuring linear accelerations, rotation rates, and orientation, all in three-axes. However, due to actuation being limited to a single axis, only four sensor measurements provided information about the motion of the pendulum tip. These are the orientation (θ obtained from magnetometers), the rotation rate (θ' obtained from a gyroscope) and normal (a_n) and tangential (a_t) acceleration components (obtained from accelerometers). For initial parameter identification experiments, only the orientation

measurements were used.

III. EQUATIONS OF MOTION

The equations of motion of the pendulum were derived using Lagrangian mechanics and are described by (1) where θ is the angle of the pendulum from vertical, L is the length of the pendulum, m is the mass at the end of the rod, x is the displacement of the actuation stage, φ is the damping coefficient, g is the acceleration due to gravity, and k is the rotational stiffness of the joint. The pendulum was assumed to consist of a point mass on the end of a massless rod.

$$\frac{d^2\theta}{dt^2} = \frac{1}{L} \cos \theta \frac{d^2x}{dt^2} + \frac{-\varphi}{L^2m} \frac{d\theta}{dt} + \frac{-g}{L} \sin \theta + \frac{-k}{L^2m} \theta \quad (1)$$

IV. IMPULSE RESPONSE FUNCTION MODEL

If the small angle assumption is made, the parameters in (1) can be lumped together, and the equation expressed by the general differential equation describing a linear second order damped system (2) where the parameters A , B , and G are found by comparing coefficients with (1), and the system input, $u(t)$, is equal to the linear acceleration, $\frac{d^2x}{dt^2}$.

$$\frac{d^2\theta}{dt^2} + A \frac{d\theta}{dt} + B\theta = Gu(t) \quad (2)$$

The parameters in (2) are described with respect to the phantom parameters in (3)-(5).

$$A = \frac{\varphi}{L^2m} \quad (3)$$

$$B = \frac{g}{L} + \frac{k}{L^2m} \quad (4)$$

$$G = \frac{1}{L} \quad (5)$$

By assuming that the initial conditions are zero, the transfer function describing the system in (2) can be derived by taking the Laplace transform of both sides and dividing the output, $\theta(s)$, by the input, $U(s)$. The transfer function is presented in (6).

$$H(s) = \frac{\theta(s)}{U(s)} = \frac{G}{s^2 + As + B} \quad (6)$$

Once the transfer function is known, the impulse response function (IRF) can be obtained using the *impz* function from the Control System Toolbox in MATLAB.

V. PARAMETER IDENTIFICATION TECHNIQUES

The geometry and mass parameters of the pendulum were measured directly and are described in Table I. The mass was assumed to be the mass of the rod and the rotational inertia of the rod was ignored. There were two unknown parameters, k and φ , in our model description that needed to be identified and different parameter estimation techniques

TABLE I
KNOWN PARAMETERS

Parameter	Value
L	0.44 m
g	9.81 m ² s ⁻¹
m	0.33 kg

Parameters of the equations of motion which were used for identifying the stiffness and damping of the system

were used.

A. Direct fit to analytical equation

The kinematics of the pendulum tip were measured during a passive decay of the phantom from a non-zero angle (0.29 rad from vertical). A solution to the model was obtained for an initial guess of the parameters. An objective function was created to minimise the RMS error between the measurements (θ_s) and the model prediction (θ_m) by fitting the parameters of the analytical model using least squares fitting. The RMS error is defined by (7) where n is the number of samples.

$$RMS = \sqrt{\frac{\sum(\theta_m - \theta_s)^2}{n}} \quad (7)$$

B. Fit to Impulse Response Function

Kinematics of the pendulum tip was measured during an impulse of acceleration experimentally approximated by rapidly decelerating the actuation stage from a constant velocity. The response was compared to the analytical impulse response function derived in MATLAB and an objective function created to minimise the RMS error between the two by fitting the parameters in (6). The equation defining the RMS error is the same as that used for fitting to the analytical equation.

VI. RESULTS

A. Fit to analytical equation

The model fit to the angle measurement using the magnetometer is shown in Fig. 2 where the best-fit damping

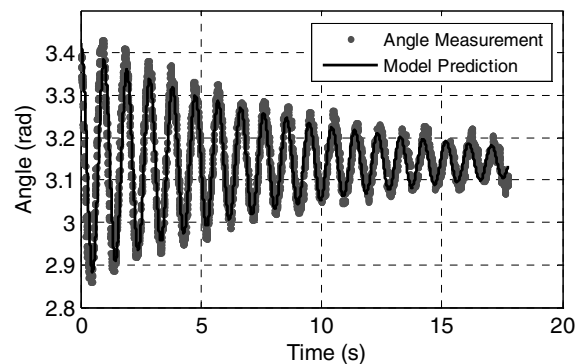


Fig. 2. Plot comparing the angle of the pendulum measured using the magnetometer and that predicted by the analytical model with the optimised parameters.

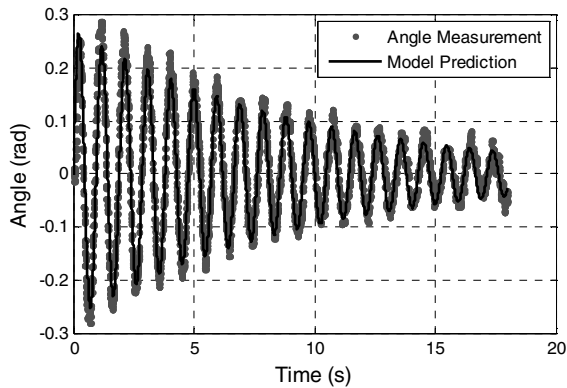


Fig. 3. Plot comparing the measured and predicted impulse response using parameters described in Tables II

TABLE II
OPTIMAL PARAMETERS BY IRF FITTING

Parameter	Value
A	0.208 s^{-1}
B	43.501 s^{-2}
G	1.802 m^{-1}

Transfer function parameters obtained when fitting impulse response to measured data

(φ) and stiffness (k) parameters were found to be $0.0142 \text{ kgm}^2\text{s}^{-1}$ and $1.396 \text{ kgm}^2\text{s}^{-2}$ respectively. The RMS error between the fit and the measurements is 0.0494 rad .

B. Fit to impulse response function

The estimate of the impulse response function and the angle measurement are shown in Fig. 3. The fitted parameters of the transfer function in (6) are provided in Table II. Using the relations in (3) and (4), the damping (φ) and stiffness (k) were found to be $0.0133 \text{ kgm}^2\text{s}^{-1}$ and $1.35 \text{ kgm}^2\text{s}^{-2}$ respectively. The RMS error between the fit and the measurements is 0.0320 rad .

VII. DISCUSSION

There are a number of limitations when constructing phantoms for research into SBS. One problem is that the infant's neck is often constructed very crudely, which limits the biofidelity of the phantom and reduces the validity of the results. It is especially important to accurately represent the motion of the neck as some research indicates that damage to the upper neck and brain stem may be a major contributing factor to the injuries of SBS [8].

This study has introduced comparative methods of objectively characterising the properties of a neck phantom, allowing for more complex phantoms to be analysed and for joint properties to be inferred *in vivo* in animal models. Obtaining estimates of joint properties, such as joint stiffness, is necessary due to the paucity of material properties available for the neck in a human infant. By having an in-depth understanding of the physical properties of the phantoms, the results can be used to investigate the

relationship between a shaking event and head motion.

There are several limitations of this research. In fitting the measurements directly to an analytic description of the equations of motion, the parameter estimates are limited by the quality of the model. As can be noticed in the model description, the stiffness and damping parameters were chosen to be linear. This was an approximation and more complex models, possibly including parameter non-linearities, need to be investigated. There is also no information as to what part of the model leads to incorrect reproduction of the kinematics of the phantom. In addition, the assumption of a linear, second order system was made when fitting to the IRF. Although the results were comparable for the simple phantom used, for more complex phantoms these assumptions may not be valid and non-linear system identification methods may be required.

There were also problems in generating an acceleration impulse. As the impulse was obtained by suddenly stopping the actuation stage, any motion caused by the preceding acceleration was retained in the system, possibly violating the assumption of steady state initial conditions. A more robust method for obtaining an estimate of the impulse response function may be to excite the phantom with a frequency rich Gaussian white noise input and to measure the resulting response. An inverse FFT of the frequency response will yield an estimation of the impulse response function [11]. Further investigation of these methods is required.

Subsequent research will include using all available sensor measurements and extending the equations of motion to represent the rotational moment of inertia in the system as currently, a massless rod is assumed. By utilising the measurements from the accelerometers and gyroscope (possibly by weighting according to the noise within each measurement), a richer description of the kinematics of the system is available. Once a single joint is accurately characterised, a series of more complex phantoms (motivated by the clinical problem) will be constructed. This will include geometry and mass properties that are representative of a human infant which will require multiple links with additional degrees of freedom. The phantoms will also need a different method of actuation which will allow the kinematics of the base and of the tip to more closely mimic the kinematics expected during shaken baby syndrome. Additional degrees of freedom in the phantom and model may result in an under-determined system if inertial measurements only on the "head" and "torso" are used. Further research will identify how complex an identifiable model describing shaken baby syndrome can be for the limited data set available.

VIII. CONCLUSION

Two techniques were used to estimate the rotational stiffness, and damping, of a 1-link inverted pendulum phantom for investigating shaken baby syndrome. The results need to be further validated before the phantom

properties can be accurately identified. Accurate results will then allow a more detailed phantom to be constructed to test methods of predicting head motion during shaking.

ACKNOWLEDGMENT

T.O. Lintern thanks the support of the Auckland Bioengineering Institute and additional funding from The University of Auckland VCSDF fund.

REFERENCES

- [1] S. Jayawant, *et al.* "Subdural haemorrhages in infants: population based study," in *BMJ (Clinical Research Ed.)*, vol. 317, 1998, pp. 1558-61.
- [2] K. M. Barlow, R. A. Minns. "Annual incidence of shaken impact syndrome in young children," in *The Lancet*, vol. 356, 2000, pp. 1571-72.
- [3] H. T. Keenan, D. K. Runyan, S. W. Marshall, M. A. Nocera, D. F. Merten, and S. H. Sinal. "A population-based study of inflicted traumatic brain injury in young children," in *The Journal of the American Medical Association*, vol. 290, 2003, pp. 621-6.
- [4] C. Hobbs, A. M. Childs, J. Wynne, J. Livingston, and A. Seal. "Subdural haematoma and effusion in infancy: an epidemiological study," in *Archives of disease in childhood*, vol. 90, 2005, pp. 952-5.
- [5] P. Kelly, B. Farrant. "Shaken baby syndrome in New Zealand, 2000-2002," in *Journal of paediatrics and child health*, vol. 44, 2008, pp. 99-107.
- [6] F. A. Bandak. "Shaken baby syndrome: a biomechanics analysis of injury mechanisms," in *Forensic Science International*, vol. 151, 2005, pp. 71-79.
- [7] S. Margulies, *et al.* "Shaken baby syndrome: A flawed biomechanical analysis," in *Forensic Science International*, vol. 164, 2006, pp. 278-79.
- [8] J. F. Geddes, H. L. Whitwell "Inflicted head injury in infants," in *Forensic Science International*, vol. 146, 2004, pp. 83-88.
- [9] J. Punt, R. E. Bonshek, T. Jaspan, N. S. McConachie, N. Punt, and J.M. Ratcliffe. "The 'unified hypothesis' of Geddes et al. is not supported by the data," in *Pediatric Rehabilitation*, vol. 7, 2004, pp. 173-84.
- [10] D. Tuerkheimer. "The next innocence project: Shaken baby syndrome and the criminal courts," in *Washington University Law Review*, vol. 84, 2009, pp. 1-58.
- [11] D. G. Manolakis, V. K. Ingle, and S. M. Kogon, *Statistical and Adaptive Signal Processing : Spectral Estimation, Signal Modeling, Adaptive Filtering and Array Processing*. Artech House, 2005.